LASER INTERFEROMETER GRAVITATIONAL WAVE OBSERVATORY
- LIGO -
CALIFORNIA INSTITUTE OF TECHNOLOGY
MASSACHUSETTS INSTITUTE OF TECHNOLOGY

Technical Note	**LIGO-T1700203–v4**	2017/10/01

Final Report: In-Vacuum Heat Switch

Adele Zawada

California Institute of Technology
LIGO Project, MS 18-34
Pasadena, CA 91125
Phone (626) 395-2129
Fax (626) 304-9834
E-mail: info@ligo.caltech.edu

Massachusetts Institute of Technology
LIGO Project, Room NW22-295
Cambridge, MA 02139
Phone (617) 253-4824
Fax (617) 253-7014
E-mail: info@ligo.mit.edu

LIGO Hanford Observatory
Route 10, Mile Marker 2
Richland, WA 99352
Phone (509) 372-8106
Fax (509) 372-8137
E-mail: info@ligo.caltech.edu

LIGO Livingston Observatory
19100 LIGO Lane
Livingston, LA 70754
Phone (225) 686-3100
Fax (225) 686-7189
E-mail: info@ligo.caltech.edu

http://www.ligo.caltech.edu/

1 Introduction

LIGO Voyager is a design concept for a next generation gravitational wave (GW) detector that is currently being developed with the aims of reaching the limits of the current LIGO facilities. One of the key upgrades is switching the substrate material for the test masses from fused silica to crystalline silicon and at the same time operating them at a temperature of 123K. At this temperature, it is possible to use amorphous silicon coatings that have lower mechanical loss and therefore generate less Brownian noise, which is limiting the current detectors. Figure 1 shows that the combined efforts of these improvements results in a broadband sensitivity improvement for LIGO Voyager, and that around 100 Hz it is most improved by a factor of five or six compared to Advanced LIGO [1].

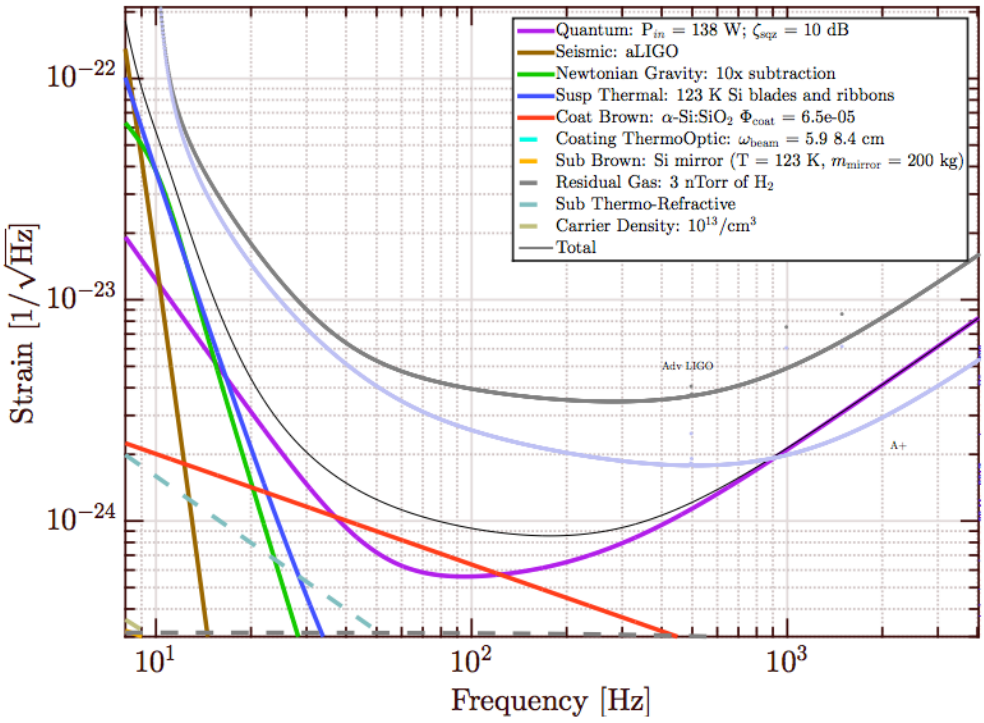

Figure 1: Expected noise budget curve for LIGO Voyager. The thermal noise from the mirror substrate (orange line) is much lower than the coating thermal noise (red line).

There are two important qualities of crystalline silicon that make it an appealing material for the LIGO Voyager mirrors. Unlike in fused silica, the mechanical losses in crystalline silicon decreases with temperature, and the thermal expansion coefficient of silicon reaches zero at 123 K [2]. Because of this property, the thermoelastic component of thermal noise can be eliminated, and thus a quieter system can be achieved. The second advantageous quality of silicon is that it has a much higher thermal conductivity than fused silica. This means that a higher power laser can be used because it is easier for the mirrors to dissipate the heat from the laser and the effects of thermal lensing are reduced [2], [3].

In operation mode, Voyager will only use radiative cooling to maintain cryogenic temperatures, but other methods of heat transfer are being considered to accelerate the initial

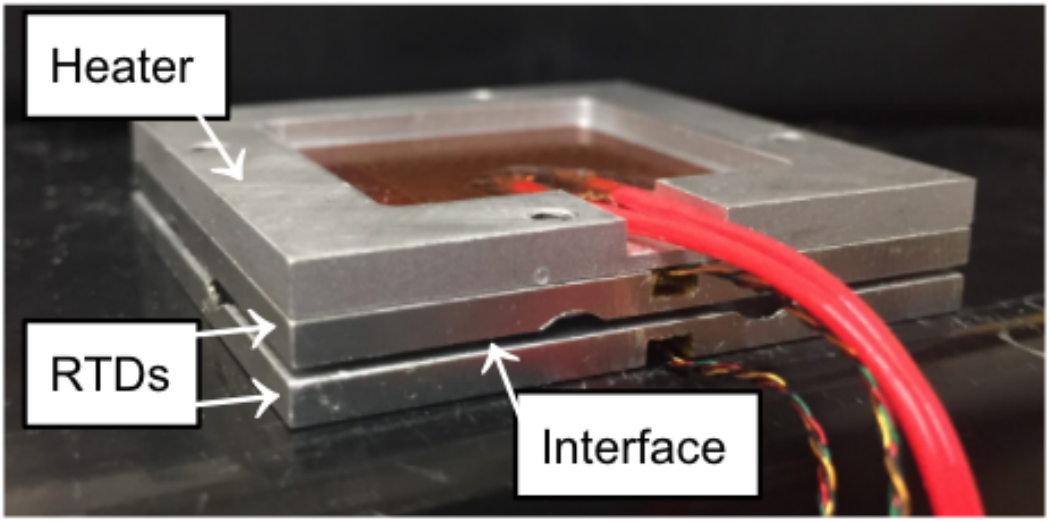

Figure 2: General assembly of how to measure the thermal conductance of a sample interface.

cooldown. Because there are strict requirements on the vacuum levels in LIGO, using an exchange gas for convective cooling is not an option. Developing a heat switch and cooling the mirrors through thermal conduction is a viable solution for an accelerated cooldown. My research for this summer was focused around studying the efficiency of heat flow across sample interfaces for different switch mechanisms. Additionally, I can use the study of heat flow to characterize the quality and strength of optically contacted samples. Optical contacting is a form of bonding where two super-polished surfaces get so close to each other that they are joined and held together by intermolecular forces [5]. Heat flow is an indicator for the effective contact area, and so it can be used to assess different switch geometries and bond qualities.

2 Experimental Setup

My experiments this summer were focused on measuring the conductance (k) of different sample interfaces and comparing them in order to understand what interfaces had better contacts or stronger bonds. It is possible to measure the conductance of an interface by placing a heating element on one side of the interface and using two temperature sensors to measure the temperature gradient that is generated across the sample, as shown in Figure 2. When the heater is supplied with a known amount of power, a temperature difference across the sample can be measured by the sensors at steady state and the conductance of the sample interface can be calculated as

$$k = \frac{Q_{SteadyState}}{\Delta T}\left[\frac{W}{K}\right] \tag{1}$$

The heater and sensor elements were placed in custom made aluminum plates in order to achieve an even distribution of heating. The aluminum plates that we ordered had a rough

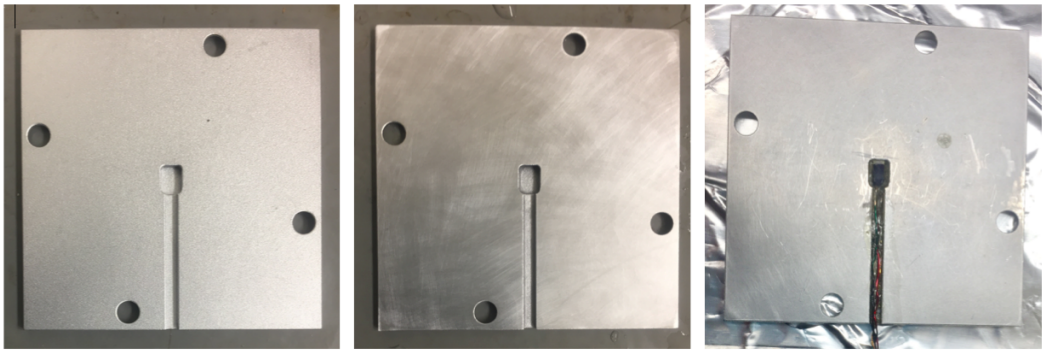

Figure 3: Left: temperature sensor plate before the sanding process. Middle: temperature sensor plate after sanding process. Right: temperature sensor glued into the plate with Lakeshore 7031 varnish.

texture to them, so I sanded each of them down to ensure the best thermal contact between the pieces. The next step was to solder two leads on either side of the sensors. This four lead setup made it possible to simultaneously supply a current and measure the resistance across the sensor with minimal contributions of lead resistances. Finally,the sensors were glued into their aluminum plates with Lakeshore 7031 varnish, which is thermally conductive and electrically insulating. Figure 3 shows the manufacturing steps of sanding the custom aluminum plates and then gluing in the sensors with the four leads. This assembly was then placed in a small cryostat that had a work plate at the bottom of the in-vacuum reservoir.

The next step was to calibrate the temperature sensors, which were 500 Ω resistance temperature detectors (RTDs). Using two of the leads, I supplied a current of 0.1 mA to each element and then used the other two leads to measure and record the output voltage at three different known temperatures: room temperature (299.25 K), freezing point of water (273.95 K), and boiling point of liquid nitrogen (77.35 K). For the cryogenic measurement, a container was filled with a small amount of nitrogen and the sensors were held just below the surface of the boiling liquid for several minutes until the measured voltage stabilized. This process ensured that the temperature measured by the RTDs was the boiling point of nitrogen, and not colder. The temperature - resistance relationship of platinum RTDs is know to be linear [9], and so a best fit line of the data allowed me to know the temperature of each RTD for a measured resistance. Figure 4 shows the calibration curves for the two sensors used in the experiment.

3 Data Analysis

After running the experiments and collecting temperature gradients for a variety of interfaces, this data could be used to accurately calculate the thermal conductances of each bond. The first step in analyzing the data was to account for the various amounts of heat loss in the system, including radiation from the aluminum plates and conductive heat transfer through aluminum plates and the sample. Once these heat losses were calculated, they were subtracted from the total 150 mW of heating power to provide a value of the steady state

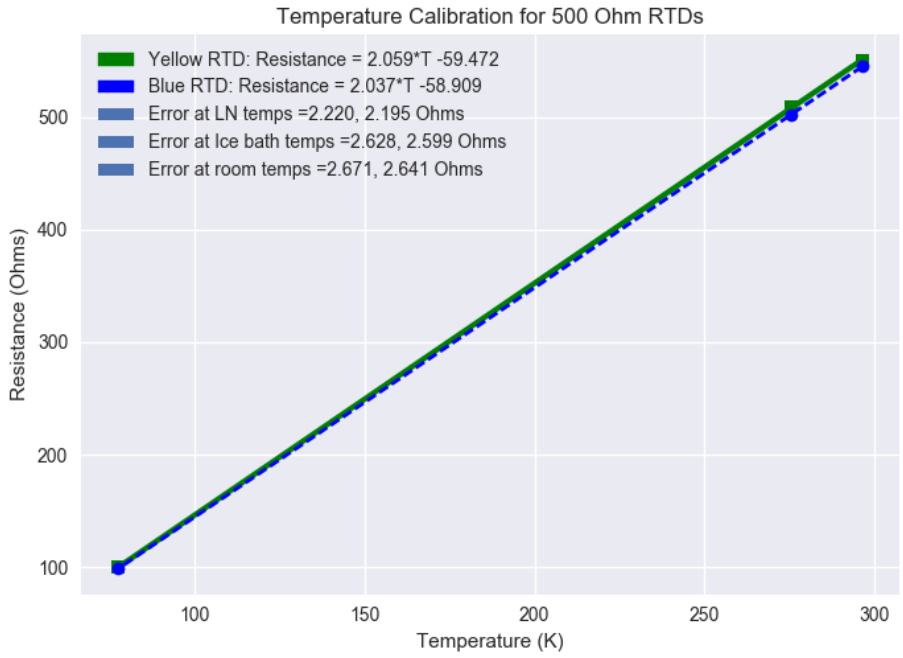

Figure 4: Temperature vs. Resistance of the two 500 Ω RTDs used in the cryostat.

heating power across just the sample interface.

One method of heat loss is radiation away from the aluminum plates. This heat loss is small, but still needs to be accounted for, and is calculated as

$$Q = \epsilon\sigma(T_{hot}^4 - T_{cold}^4)A \tag{2}$$

where ϵ is the emissivity of the material, σ is Stefan-Boltzmann constant, and A is the area of the material. T_{hot} was the extrapolated temperature measured by the RTD next to the heater, and T_{cold} was the temperature of the cryostat, which is the temperature measured by the RTD before the heater is turned on. The emissivity of aluminum is about 0.06, and the plates had dimensions of 1.5 inches by 1.5 inches. The heat loss due to radiation was no more than 0.006 W, or 4% of the supplied heating power of 150 mW.

A second heat loss mechanism comes from the heat transferred to the steel weight on top of the assembly, as seen in Figure 6 and then radiating away from it. At steady state, the steel mass will be the same temperature as the heater, and will be radiating away heat into the surrounding atmosphere, which is at a lower temperature. In order to keep the steel mass at a constant temperature, the heater must dump a portion of its total heating power into the steel mass. This is a similar calculation as described above, but with different values for the emissivity and surface area. This had a maximum value of about 0.015 W, or 10% of the supplied heating power of 150 mW. These heat losses were subtracted from the supplied power of the heater and this new value was used as the steady state heating power of the system.

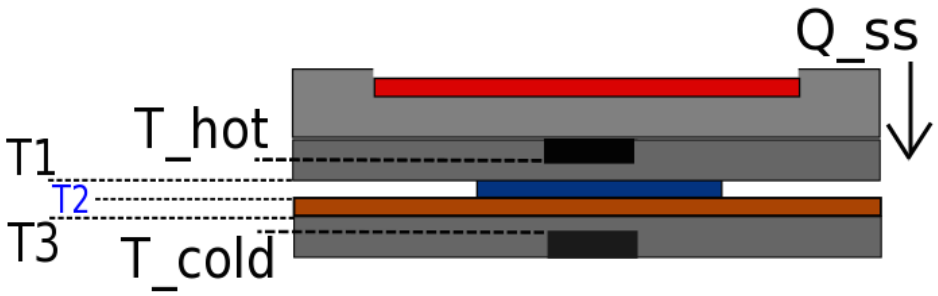

Figure 5: Schematic of the copper - silicon interface. T_hot and T_cold are the temperatures measured by the RTDs. T1 and T3 is the temperature gradient across the sample.

$$Q_{SteadyState} = 150\,\mathrm{mW} - Q_{AluminumRadiation} - Q_{SteelRadiation} \tag{3}$$

Now that the steady state heating power of the system is known, it is possible to make more accurate conductance calculations. Figure 5 shows a side view schematic of the copper - silicon interface. The temperature sensors measure T_{hot} and T_{cold}, so to find the temperature gradient across only the sample interface (T1 and T3), it is necessary to account for the heat lost due to conduction through the aluminum plates. The thermal conduction equation is

$$Q = \frac{\lambda A(\Delta T)}{d} \tag{4}$$

where λ is the conductivity, A is the area, and d is the thickness of the material. Since the conductivity of aluminum is known for different temperatures, and the steady state heating power ($Q_{SteadyState}$) is calculated using Equation 3, it is possible to solve for the unknown temperature at the surface of the aluminum plates.

The final step is to solve for the conductance of the bond interface. This calculation is relatively straightforward since conductances add inversely in series, and the conductivity and dimensions of our sample interfaces are known.

$$\frac{1}{k_{sample}} = \frac{1}{\lambda_{silicon} \cdot \frac{A_s}{d_s}} + \frac{1}{\lambda_{copper} \cdot \frac{A_c}{d_c}} + \frac{1}{k_{bond}} \tag{5}$$

By comparing the conductances of similar interfaces, it was possible to make conclusions about the relative strength or quality of the contact.

4 Types of Tested Interfaces

The experimental setup and data analysis process that I outlined above can be applied to a wide variety of sample interfaces. This summer I focused my attention on two main interfaces that have possible applications in LIGO Voyager and are described in more detail below.

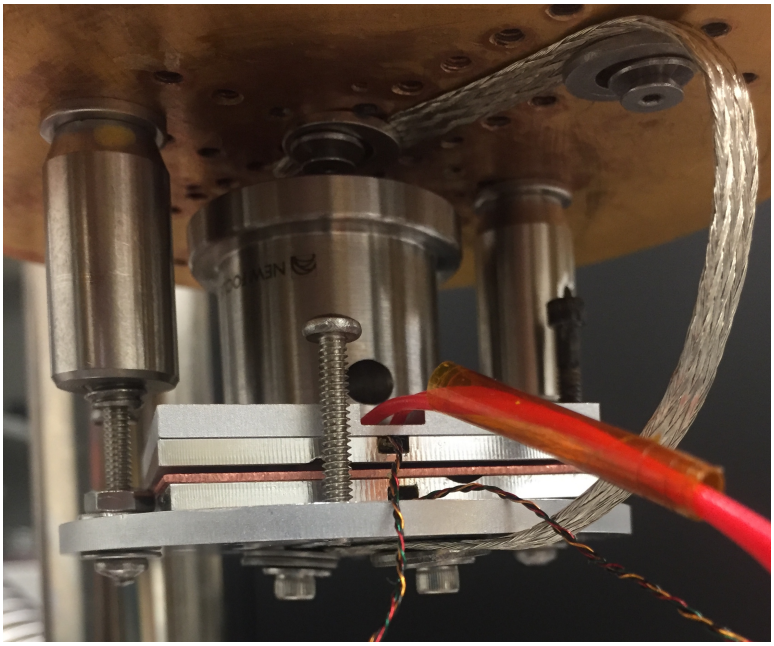

Figure 6: Assembly of temperature sensors, heater and samples on the cryostat cold plate. There is a stainless steel cylinder on top of the assembly in order to keep stack from sliding around during the experiment. A thermal strap connects the coldplate to the working plate to supply faster cooling.

4.1 Copper - Silicon Interface

The first interface I investigated was between copper and silicon, which models a potential solution of the LIGO Voyager clamping mechanism. There were three copper plates available with different surface finishes: mirror, polish, and brush, and I was interested in determining if the type of finish impacted the efficiency of heat transfer between the copper and silicon samples. Since copper oxidizes in air, it was essential to remove this layer of contamination before performing the experiments in order to ensure the best possible contact between the samples. A simple but effective way of cleaning copper is to place the samples in a boiling solution of salt, vinegar and water for about ten minutes [4]. After the samples were thoroughly cleaned, I assembled the temperature sensors, heater, and interface on the work plate as shown in Figure 6 and then cooled the cryostat down to liquid nitrogen temperatures. Once the system reached its minimum temperature, I turned on the heater and measured the temperature gradient across the interface as it neared steady state.

4.1.1 Clamping Mechanism

As an additional and more realistic way of measuring conductive heat flow, I designed a clamping mechanism in SolidWorks that attaches to the coldplate of the cryostat and can be opened and closed using a rotary feedthrough and system of gears. This mechanism would model a potential heat switch used in LIGO Voyager and could provide information on how the time constant changes when the clamp is engaged versus when it is disengaged. A screenshot of my design is shown in Figure 7. I created a 3D printed version of this model,

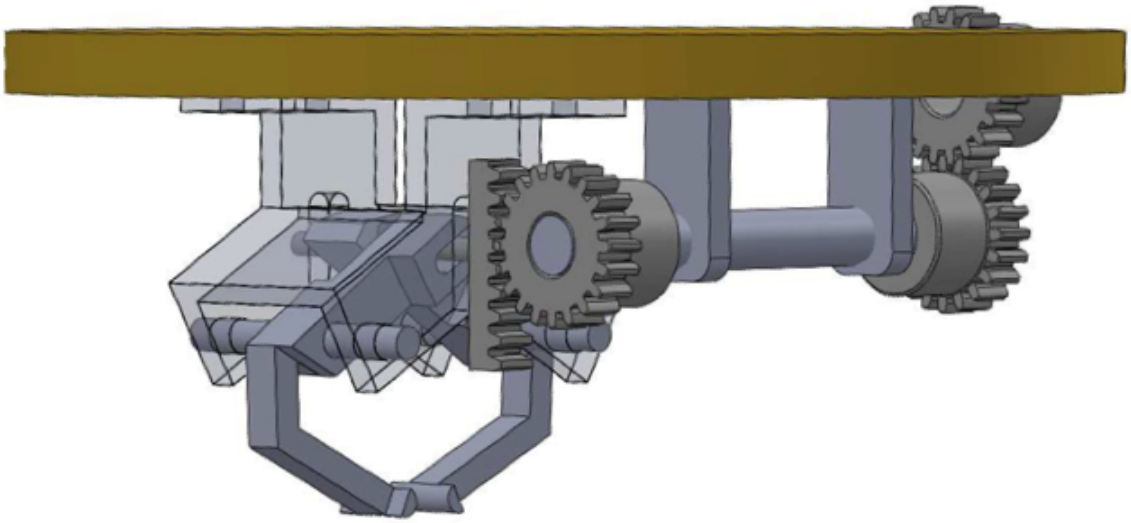

Figure 7: First prototype of a clamping mechanism that will attach onto the cold plate. Rotary feedthrough and silicon sample are not pictured.

which allowed me to discover shortcomings of the design and make appropriate adjustments to the drawing. Unfortunately due to lead times, I was unable to send the final design to a machine shop to be fabricated.

4.2 Interface 2: Optical Contacting

The second type of interface I created and tested was between two optically contacted silicon pieces. Also called direct bonding, optical contacting can be achieved when the surfaces of two samples are clean enough and smooth enough to be bonded through inter-molecular forces when placed in contact with each other. The silicon wafers that I used in my experiment were 500 μm thick and came in squares of both 4 cm^2 and 1 cm^2. I cleaned and contacted these samples using the following process:

1. Use the ion gun to blow off any large particles from the surface.
2. Apply a thin layer of First Contact solution and once it has dried, peel it off slowly while using the ion gun to neutralize any resulting charge separation.
3. Once the surfaces are clean, make a right angle with two blocks and put one silicon piece flush against the corner.
4. Place the second piece (clean side down) on top of the first piece, as shown in Figure 8, and push down to form the bond. This procedure is known as "ansprengen."

First Contact, which is used in LIGO to clean the sensitive interferometer optics, is a blend of polymers and solvents that is applied as a liquid by brush or spraying and leaves a polymer film behind that can be peeled off, removing contaminants from optical surfaces [8]. During

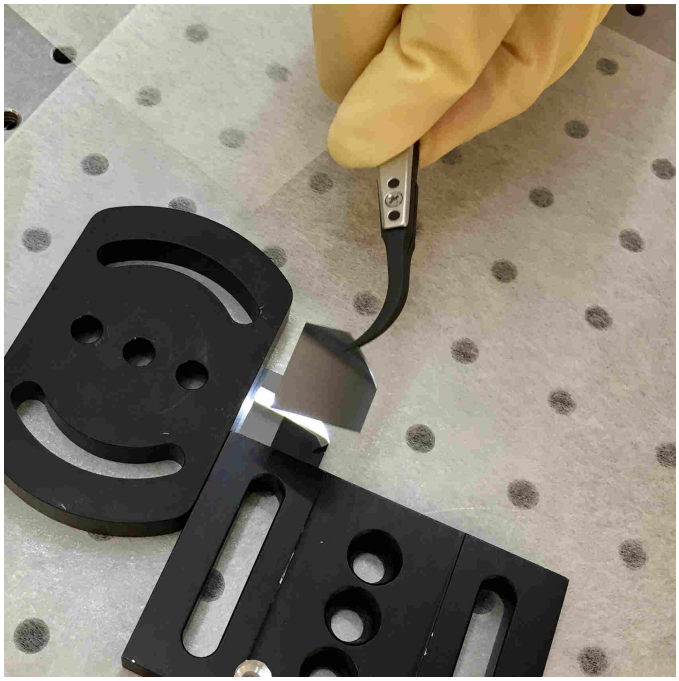

Figure 8: Process of optically contacting two silicon wafers.

the first attempts at contacting, I was able to contact both sides of the wafer to create a stack of three optically bonded samples. However, for the experiments that I conducted, I only investigated a single optical bond. I created five bonded samples using the procedure described above, and applied different amounts of heat and pressure to each of these samples. Then I used the experimental setup in my cryostat to measure the conductance for each of the samples and compared how their curing methods impacted the strength of their optical bond. I operated these experiments at room temperature to save time.

5 Results

For all of the experimental runs, the heater was supplied with 150 mW of power, the RTDs were each supplied with 5 mA of current and the output voltage was recorded by a data acquisition system. The time constants of the temperature curves were very large, so instead of waiting for the system to reach steady state, I recorded enough data to be able to generate an exponential best-fit line, and from this equation I extrapolated the final temperature of each RTD. This procedure saved time and allowed me to run experiments on more interfaces. Figure 9 shows the full data recorded by the RTDs from the interface of the silicon and brushed copper finish sample. An exponential fit to the entire data is not an accurate representation of the steady state process, especially in the first few hours of data collection. This is because immediately after the heater is turned on, there are background processes, such as parts heating up and acting as transient heat sinks, that are occurring along with the conductive heat transfer through the sample. In order to account for this "burn in" period, I have eliminated the first several hours of data and fit the exponential curve to the

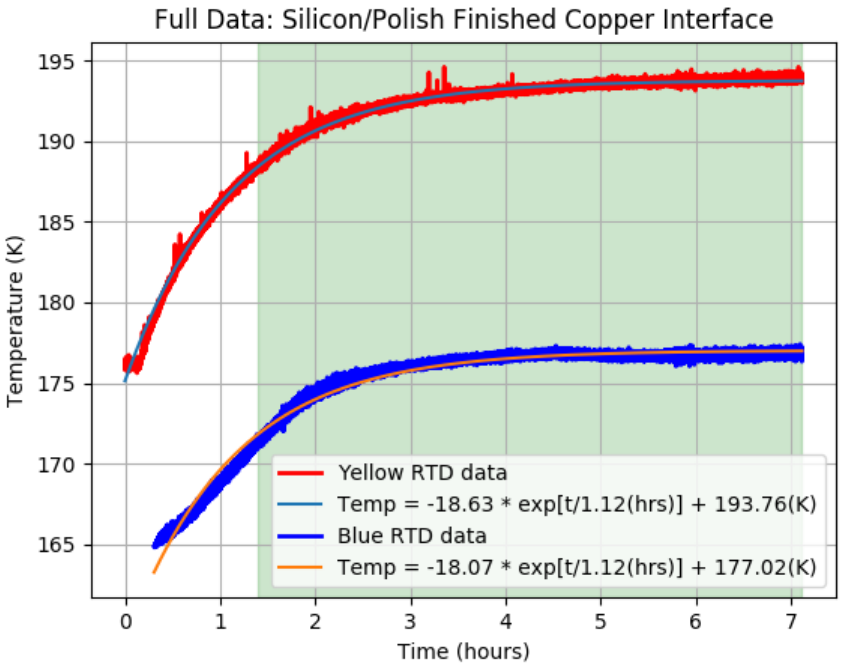

Figure 9: Full data collected from both RTDs for the sample interface of polished copper and silicon, with an exponential fit applied. It is a poor fit, especially in the first several hours of data collection. The shaded green region is the data that I used for my calculations, shown in Figure 10.

remaining data, as shown in Figure 10. From these exponential fits, I extrapolated the final temperatures that each RTD would reach.

These extrapolated steady-state temperatures were used to calculate the temperature gradient across just the interface, using Equation 4. This new value for ΔT was then plugged into Equation 1 to calculate the conductance of the entire interface. In order to get just the conductance of the bond, Equation 5 was used to subtract away the contributions from the silicon and copper wafers. From this equation, it is possible to solve for k_{bond} for each sample interface. The results are listed below in Table 1.

A similar data analysis procedure was used on the silicon optically bonded samples, and the results are listed below in Table 2.

6 Conclusion and Future Work

Table 1 shows that a more polished surface results in a higher bond conductance, which indicates a better contact between the silicon and copper samples. This agrees with basic intuition because polished surfaces have more potential contact points than rougher surfaces. Since this interface models the interface seen by the heat switch and test mass, an important next step would be to investigate the relationship between contact quality and applied force.

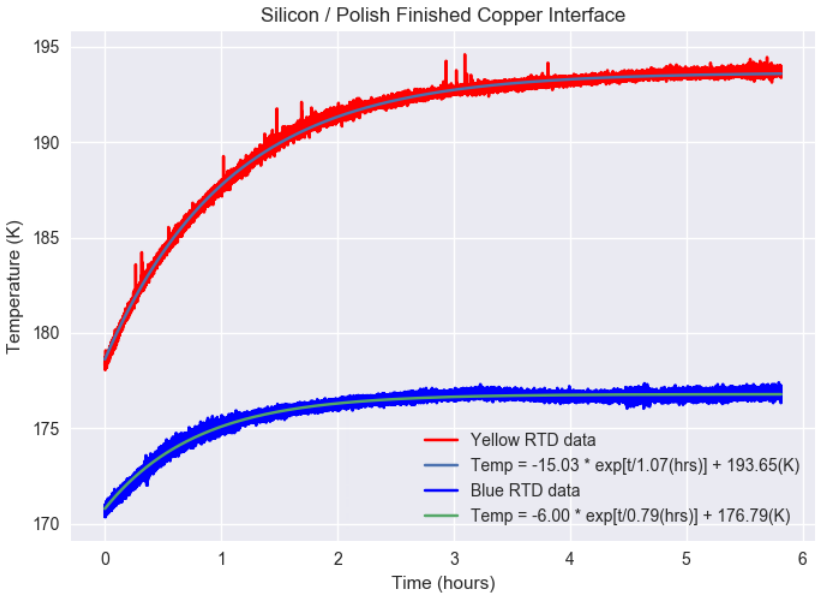

Figure 10: Data collected from both RTDs after the 'burn in' period, with an exponential fit applied. Final temperatures of each RTD were calculated from these best fit lines.

Type of Copper Finish	**Thermal Conductance (W/K)**
Brush	0.00501 ± 0.00041
Polish	0.00748 ± 0.00063
Mirror	0.00921 ± 0.00078

Table 1: Bond conductance of copper - silicon interfaces.

Sample Curing Process	Thermal Conductance (W/K)
325°C, 3 kg	0.1048 ± 0.0335
35°C, 1 kg	0.0512 ± 0.0090
275°C, no weight	0.0518 ± 0.0090
No heat, 2.25 kg	0.0492 ± 0.0082
No heat, no weight	0.0375 ± 0.0052

Table 2: Bond conductance of the silicon optically contacted samples. The two samples that were heated and under pressure had dimensions of 1cm x 1cm, while the three baseline samples had dimensions of 2cm x 2cm.

Table 2 shows that curing the samples with both heat and pressure increases the bond conductance, and thus strengthens the optical contact. The only heated sample and the only weighted sample were both an improvement over the null sample, which indicates that both pressure and heat are important for a strong bond. Table 2 also agrees with previous research on annealing silicon optical bonds that show that below 300C there is not a significant change in the resulting bond strength, whereas above 300C, the bond strength increases steadily, before eventually leveling off at about 1000C [6]. Unfortunately, there has been little research on how pressure impacts silicon optical bond strength, and so this should be a focus for future experiments, since it appears that pressure does lead to a stronger bond. The results from my two experiments align with basic intuition and prove that it is possible to use thermal conductance as a measurement of bond strength or contact quality. However, the nature of these temperature conductivity tests is that individual data points take a long time to record, which limited how much of the parameter space could be explored with corresponding samples. Future work using a similar experimental setup can provide more information about how to create a high quality heat switch interface and how to cure an optical contact to produce the strongest bond.

- **Optical Contacting:** The next step in this experiment would be to determine what amount of applied heat and pressure produces the strongest optical contact. Applying too much heat might damage the silicon substrate and thus weaken the bond, while applying applying excess weight is unlikely to damage the bond but could be unnecessary.

  There is a second way of measuring optical bond strength that should be investigated. This method involves forcing a razor blade into the bond, which would open up a gap of length L, shown in Figure 11. From this length, it is possible to directly calculate the bond strength of the optical contact with the equation

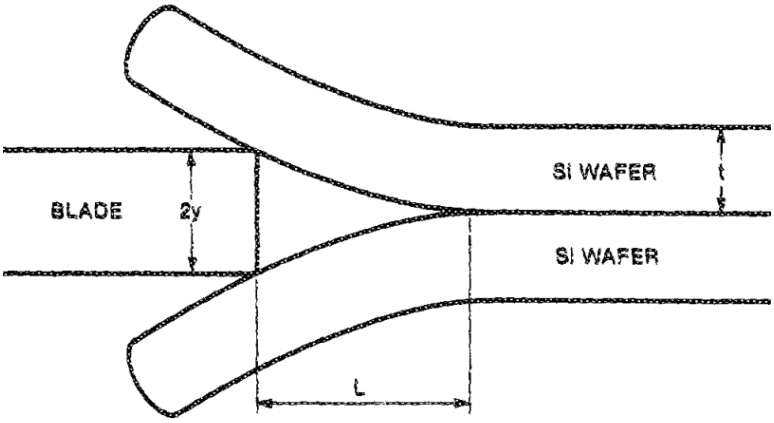

Figure 11: Schematic of the razor blade method of determining bond strength [10].

$$\gamma = \frac{3}{8}\frac{Et^3y^2}{L^4} \tag{6}$$

where E is the modulus of elasticity of silicon, and L, t, and y are the dimensions shown in Figure 11 [10], [11]. When applying this method, it is important to have fine control over the position of the razor blade, in both the vertical and horizontal directions, as well as rotational. It would be ideal to develop a clamp that can attach to a translation stage and that can change the angle of the blade until the blade is perfectly aligned with the interface. Additionally, the clamping force should focus on the blade instead of the handle and should cover as much area as possible. This will prevent the blade from buckling when it comes into contact with the optically bonded sample. In order to help with the placement of the blade and to measure all of the desired distances, a microscope or other type of magnifying system should be set up along with a camera to capture side images of the opened gap (a USB microscope might be a good option). Once the blade is inserted and a gap is opened, the known thickness of the silicon wafer can be used to calibrate the gap images and the required separation and gap depth can be extracted. From this information, all other dimensions can be measured and plugged into Equation 6. With enough measurements, it should be possible to establish a relationship between the thermal conductance and the bond strength γ of an optically contacted bond.

- **Copper - Silicon Interface:** It is important to understand how much force will need to be applied in the clamping mechanism to reach maximum efficiency of heat transfer. This relationship can be determined by stacking more weight on top of the interface and measuring the respective thermal conductance. There will be a point where stacking more weight will not significantly increase the conductance of the interface, and it is this amount of force that will need to be applied by the clamping mechanism. Another concern is damaging the test mass, since the geometry will be quite different and the masses will need to be touched by individual 'fingers.' Too much force on this localized contact can easily damage the brittle silicon.

- **Clamping Mechanism:** The next step for this project is to send the clamping mechanism design to a machine shop to be fabricated and then assemble the gears and mechanism onto the coldplate. In order to ensure that it is working correctly, the system should be tested in open air before closing the cryostat and cooling it down to liquid nitrogen temperatures. A lever attached to the rotary feed through can be used to measure the amount of torque that the clamping mechanism is applying on the silicon sample. This experiment can provide a more realistic representation of how the clamping mechanism will operate and transfer heat in LIGO Voyager.

References

[1] https://dcc.ligo.org/DocDB/0112/T1400226/008/main.pdf

[2] B. Shapiro *et al.*, *Cryogenically Cooled Ultra Low Vibration Silicon Mirrors for GW Observatories*. https://dcc.ligo.org/public/0138/P1600301/006/P1600301-v6.pdf

[3] S. Rowan *et al.*, *Test mass materials for a new generation of gravitational wave detectors* Proc. of SPIE Vol. 4856, (2003)

[4] L. D. Rosenhein, *The Household Chemistry of Cleaning Pennies* Journal of Chemical Education Vol. 78, No. 4 (2001)

[5] JJ Ferme, *Optical Contacting* Proc. of SPIE Vol. 5252, (2003).

[6] M. A. Schmidt, *Silicon Wafer Bonding for Micromechanical Devices* Solid-State Sensor and Actuator Workshop, pp. 127-13 (1994).

[7] L. Klobučar *Thermal radiation heat transfer between surfaces* http://mafija.fmf.uni-lj.si/seminar/files/2015_2016/Thermal_radiation_heat_transfer_between_surfaces_Luka_Klobucar.pdf

[8] https://www.photoniccleaning.com/

[9] National Physics Laboratory *Platinum Resistance Thermometer* http://www.npl.co.uk/reference/faqs/what-is-a-platinum-resistance-thermometer-(faq-thermal)

[10] W. P. Maszara *et al.*, *Bonding of silicon wafers for silicon-on-insulator* Journal of Applied Science Vol. 64, (1988)

[11] P. P. Gillis, J. J. Gilman, *Double-Cantilever Cleavage Mode of Crack Propagation* Journal of Applied Science Vol. 35, No. 3 (1963)